Domain Shared and Specific Prompt Learning for Incremental Monocular Depth Estimation

Anonymous Authors

ABSTRACT

Incremental monocular depth estimation aims to continuously learn from new domains while maintaining their performance on old domains. The catastrophic forgetting problem is the key challenge when the model adapts the dynamic scene variations. Previous methods usually address this forgetting problem by storing raw samples from the old domain, allowing the model to review the knowledge of the old domain. However, due to the concerns of data privacy and security, our objective is to tackle the incremental monocular depth estimation problem in more stringent scenarios without the need for replaying samples. In this paper, we attribute the cross-domain catastrophic forgetting to the domain distribution shifts and continuous variations of depth space. To this end, we propose **D**omain **S**hared and **S**pecific **P**rompt Learning (DSSP) for incremental monocular depth estimation. In detail, to alleviate the domain distribution shift, complementary domain prompt is designed to learn the domain-shared and domain-specific knowledge which are optimized by the inter-domain alignment and intra-domain orthogonal loss. To mitigate the depth space variations, we first introduce a pre-trained model to generate the domain-shared depth space. Then, we design S^2-Adapter that quantizes depth space variations with scale&shift matrices and converts the domain-shared depth space to domain-specific depth space. Our method achieves state-of-the-art performance under various scenarios such as different depth ranges, virtual and real, different weather conditions, and the few-shot incremental learning setting on 12 datasets. We will release the source codes and pre-trained models.

CCS CONCEPTS

• **Computing methodologies** → **Computer vision**; **Lifelong machine learning**; **Scene understanding**.

KEYWORDS

Monocular depth estimation, incremental learning, domain prompt learning

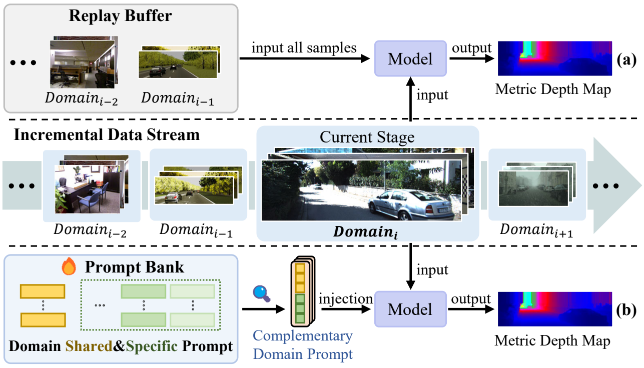

Figure 1: Overview of our method (b). Compared with typical approaches (a) that rely on rehearsal buffers to alleviate forgetting, DSSP mitigates domain distribution shifts and depth space variations through the complementary domain prompt and S^2-Adapter.

1 INTRODUCTION

Monocular depth estimation aims to generate dense depth maps from a single RGB image, which is an important scene perception technique. In practice, new domains substantially emerge with environmental variations, such as weather and illumination conditions. Incremental monocular depth estimation intends to facilitate continuous learning and adaptation of the model in such dynamic environments while maintaining its depth estimation performance in the old domain.

In incremental monocular depth estimation, the catastrophic forgetting problem is the key challenge that is caused by domain distribution shifts and depth space variations. 1) Each domain has a unique data distribution corresponding to the environmental factors, which leads to severe domain gaps among them. Consequently, when the model adapts to a new domain, the shift of feature distribution leads to the phenomenon of forgetting old knowledge. 2) Different domains usually have different depth ranges and spatial structures, so the depth space exhibits scale and shift variations across domains. When the model adapts to these variations on new domains, it may result in the forgetting of old knowledge.

To address the aforementioned problems, some approaches [28, 29] attempt to reduce the domain gaps by employing multi-domain learning across as many domains as possible and alleviate the influence of the depth space variations by predicting relative depth maps. However, exhaustively covering all domains in the real world is impractical, and retraining the model from scratch consumes plenty of time and computational resources. Other methods [6, 11, 40] try to continuously fine-tune the model and ease the forgetting problem by maintaining a replay buffer involving samples from old domains which enables the model to review them while learning new knowledge. Such as LL-MonoDepth [11] stores 500 samples in each domain for reviewing old knowledge while employing multiple predictors to adapt the depth space variations on different domains. However, storing samples may not always be feasible, especially for scenarios where long-term storage of data is not permitted owing to privacy or data use legislation [34]. Therefore, we aim to address the incremental monocular depth estimation in a more strict protocol without the need for replay samples.

Recently, pre-trained models embed knowledge into enormous parameters, and this empowers them with a better capability of mitigating forgetting. Researchers leverage prompt learning with pre-trained models to learn task-specific knowledge in the new domain. Inspired by this, we introduce learnable prompts to capture and retain domain-specific knowledge, which represents domain distribution information through several parameters, thereby saving storage costs and avoiding concerns of data privacy and security. Furthermore, prompts can also learn unified feature representations across domains to reduce domain gaps and enhance the generalization capability of the model.

Therefore, we propose **D**omain **S**hared and **S**pecific **P**rompt Learning (DSSP) for incremental monocular depth estimation, which designs complementary domain prompts and Scale&Shift Adapters (S^2-Adapter) to mitigate domain distribution shifts and depth space variations. Specifically, we first design domain-shared prompts to continually learn across all domains and prevent knowledge forgetting by domain shift through inter-domain alignment constraint, while we design domain-specific prompts solely to learn in the corresponding domain to enhance the adaptability of the model and retain knowledge in their parameters. Additionally, we introduce an intra-domain orthogonal loss to constrain these two types of prompts to focus on the unified inter-domain representation and individual domain distribution respectively. Both two types of prompts are maintained in the prompt bank. Therefore, we leverage the frozen pre-trained model with the complementary domain prompts to predict a relative depth map. Furthermore, to capture the depth space variations and convert the relative depth into metric depth, we devise the lightweight S^2-Adapter which precisely learns the map between the relative depth and metric depth through quantifying depth space variations into scale&shift matrices. As illustrated in Figure 1, in contrast to previous replay-based methods, DSSP generates complementary domain prompts by learning domain-shared prompts and domain-specific prompts, facilitating the learning of new knowledge while retaining previous knowledge without data privacy and security concerns.

During the inference phase, we predict the domain of the test image according to the domain-specific prompt. Then, we generate complementary domain prompt and subsequently inject them into the pre-trained model to predict the relative depth map. Next, the S^2-Adapter is selected by the domain identity to restore the depth space transformation and predict the final depth. Experiments on 12 datasets demonstrate our DSSP outperforms the SOTA methods.

The main contribution of our work can be summarized as follows:

- We propose domain shared and specific prompt learning to alleviate the catastrophic forgetting problem of incremental monocular depth estimation without data privacy and security concerns.
- We devise a S^2-Adapter which quantifies depth space variations into scale&shift matrices to capture the map between relative depth and metric depth and mitigate the influences of depth space variations.
- Extensive experiments on multiple domain incremental sequences show our method achieves superior incremental monocular depth estimation performance.

2 RELATED WORK

2.1 Monocular Depth Estimation

As a technique for scene perception, monocular depth estimation aims to generate per-pixel depth maps for scenes based on a single RGB image. Previous learnable methods achieve satisfactory performance through supervised [1, 9, 12, 14, 15, 19, 21, 27], self-supervised [10, 20, 24, 39, 42, 51] and unsupervised learning [36, 49, 50, 52] on single domain. However, due to the lack of robustness and generalization, models usually exhibit poor performance in new domains when they are applied in the real world. Some works tend to collect a large scale of data samples across various domains and learn a domain-invariant model [29, 37, 43, 46, 47]. However, it is impossible to cover all domains in practical applications. Therefore, when a new domain emerges, the model has to combine the data of the new domain with all old domains and be retrained from scratch, which is time-consuming. Meanwhile, the large number of parameters in these pre-trained models makes training them from scratch expensive in computing resources. To address the above problem, researchers devote numerous efforts to exploring incremental monocular depth estimation methods, so that the model can continuously adapt to the new domain without forgetting the knowledge of the old domain. Recently, some researchers try to store a part of samples of old domains and maintain a replay buffer that allows the model to access when fine-tuning on the new domain. Although the model alleviates the catastrophic forgetting problem by reviewing these replay samples, it is not practical to store data for a long time due to data privacy and security concerns in many real-world scenarios.

2.2 Incremental Learning

Incremental Learning is a typical setting to continuously train a single model on non-stationary data distributions. The major challenge is the catastrophic forgetting problem [26], where adaptation to a new distribution usually results in a much-reduced ability to capture the old distribution. Inspired by the complementary learning systems (CLS) theory [18, 25], researchers devote numerous efforts to facilitating the model to learn from continuous data streams, such as storing some training samples for each of the previous tasks and reusing them while learning a new task (replay methods) [2, 3, 5, 23, 30, 41, 48]; imposing extra regularization instead of storing training samples (regularization-based methods), such as LwF [22] using a knowledge distillation loss on previous tasks and EWC [17] enforcing an additional loss term to alleviate changing on the weights important for previous tasks; fixing trained parameters on old tasks and employ extra network branches for training a new task (parameter isolation methods) [16, 31, 33, 44]. These methods are empirically demonstrated useful for image recognition [16, 17, 41], while they mainly focus on the class-incremental problem. Directly transferring these methods to incremental monocular depth estimation may face two challenges, domain distribution shifts and depth space variations.

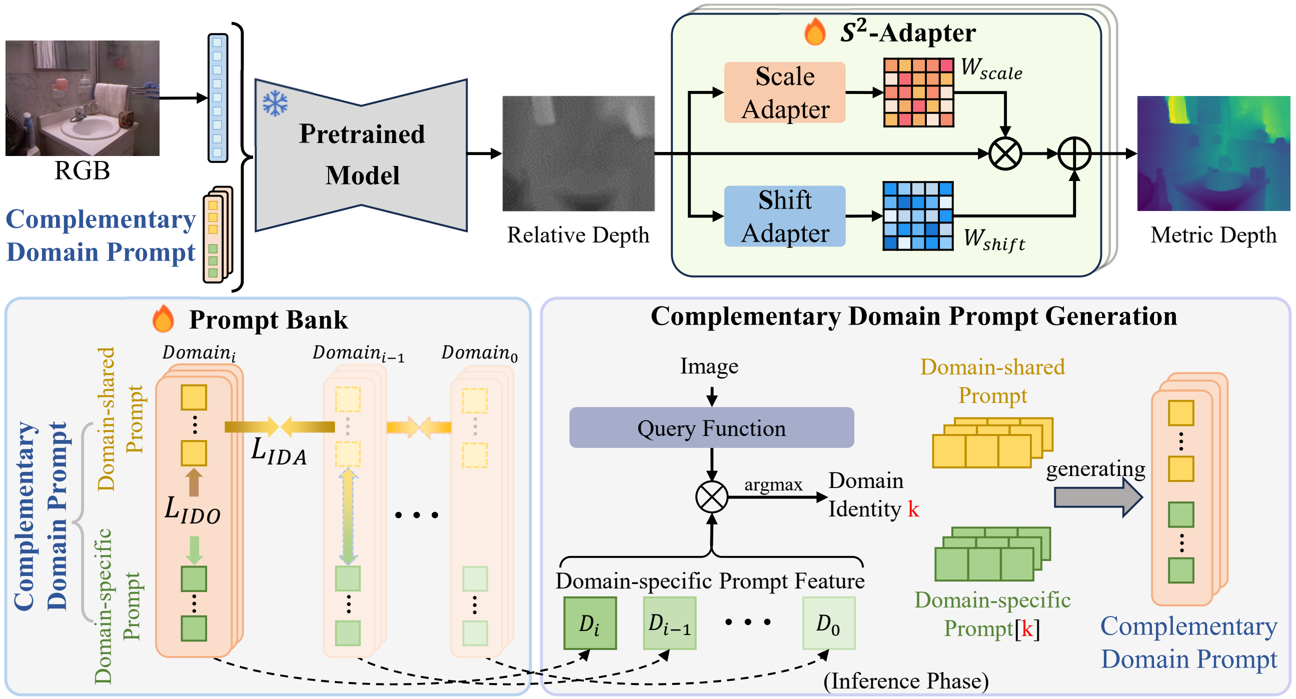

Figure 2: Overview of the proposed network architecture. We propose domain shared and specific prompt learning for alleviating domain distribution shifts and S^2-Adapter for adapting the depth space variations.

3 MYTHOLOGY

In this section, we first introduce the paradigm of incremental monocular depth estimation tasks. Then, we overview our pipeline during both the training and inference phases. Next, we describe the complementary domain prompt learning strategy. Furthermore, we detail the S^2-Adapter. Finally, we elaborate on inferring the domain identity of the test images for the generation of complementary domain prompt and the selection of S^2-Adapter.

3.1 Incremental Monocular Depth Estimation

In this task, the data of different domains are incrementally obtained. We define a sequence $\mathcal{D}$ with S domains, $\mathcal{D} = \{\mathcal{D}_1, \cdots, \mathcal{D}_S\}$. In the s-th domain $\mathcal{D}_s = \{(x_i^s, y_i^s)\}_{i=1}^{N_s}$, there are N_s images $x_i^s \in \mathcal{X}^s$ and its corresponding depth map $y_i^s \in \mathcal{Y}^s$. Given an image x from arbitrary domains, our goal is to train a single model $f_{\theta_s} : \mathcal{X}^s \to \mathcal{Y}^s$ parameterized by θ_s to predict the depth map $\hat{y}$ denotes as $\hat{y} = f_\theta(x)$. Generally, the model f_{θ_s} is optimized by,

$$\mathcal{L} = \mathcal{L}_d(y, \hat{y}) + \mathcal{R} \tag{1}$$

where $\mathcal{L}_d$ is the depth estimation loss to learn the knowledge on the new domain, and $\mathcal{R}$ is a regularization loss for preserving the knowledge from old domains. Our method tackles the more challenging incremental monocular depth estimation which data from previous domains are not be seen anymore.

3.2 Overview

In incremental monocular estimation, the catastrophic forgetting problem is caused by continuous domain distribution shifts and depth space variations. To this end, we propose DSSP, which is composed of complementary domain prompt and S^2-Adapter. As illustrated in Figure 2, we maintain a prompt bank containing learnable prompts throughout all incremental stages. The complementary domain prompt, along with image embedding, is fed into the frozen pre-trained depth estimation model and then yields a relative depth map. We froze the pre-trained model to prevent it from the influenced by domain distribution variations. Subsequently, following adjustments in scale and shift by our S^2-Adapter, the relative depth map is transformed into the final metric depth map. In the inference phase, we first infer the domain identity of the input image, thereby generating the complementary domain prompt and selecting the S^2-Adapter based on the domain identity. Finally, based on the domain distribution knowledge within the prompt and the depth space rule within the S^2-Adapter, we can continuously estimate the depth map accurately with less forgetting. During all incremental learning stages, only the complementary domain prompt and the S^2-Adapter are trainable, which only cost less than 1M parameter per domain.

3.3 Complementary Domain Prompt Learning

To address the issue of forgetting in incremental monocular depth estimation, previous methods store raw samples from the old domain and input them alongside samples from the new domain into the model. These approaches allow the model to review knowledge from the old domain while learning from the new domain. However, in many real-world scenarios, data from the old domain may not be retained and accessed in the long term due to privacy and security concerns. Therefore, instead of directly storing raw samples of each domain, we introduce learnable prompts to capture and store domain knowledge. These learnable prompts can explore the individual features of each domain, enhancing the adaptability of pre-trained models. Meanwhile, these prompts can also mine inter-domain common knowledge through long-term learning to improve the cross-domain generalization of the model. Overall, the prompts can not only learn the characteristics of each domain but also model generic information across domains, thereby mitigating the catastrophic forgetting problem without data privacy and security concerns.

Based on the aforementioned analysis, we devise complementary domain prompt learning, which consists of domain-shared prompt and domain-specific prompt to learn both domain-general knowledge and domain-specific knowledge for each domain respectively. Given a pre-trained model with M transformer layers in which the embedding dimension of the hidden layer is d, we learn M domain-shared prompt $\mathbf{P}_{shared}$ and domain-specific prompt $\mathbf{P}_{specific}$:

$$\mathbf{P}_{shared} = \{p^i_{shared} \in \mathbb{R}^{l_p \times d} | 0 \leq i \leq M-1\}; \quad (2)$$

$$\mathbf{P}_{specific} = \{p^i_{specific} \in \mathbb{R}^{l_p \times d} | 0 \leq i \leq M-1\} \quad (3)$$

where l_p is the length of prompts. Then, we generate the complementary domain prompt $\mathbf{P}_{comp} = \{p_i \in \mathbb{R}^{2*l_p \times d} | 0 \leq i \leq M-1\}$ by:

$$\mathbf{P}_{comp} = [\mathbf{P}_{shared}, \mathbf{P}_{specific}], \quad (4)$$

where $[\cdot, \cdot]$ denotes the concatenation along the length dimension. Next, we inject the complementary domain prompt $\mathbf{P}_{comp}$ into the first transformer layer L_1 of the pre-trained model alongside the image embedding e which is extracted by the input image I:

$$[cls_1, \_, h_1] = L_1\left([cls_0, p_0, e]\right), \quad (5)$$

Subsequently, the rest complementary domain prompt is injected into the pre-trained model with each hidden embedding feature:

$$[cls_i, \_, h_i] = L_i\left([cls_{i-1}, p_{i-1}, h_{i-1}]\right) \quad i = 2, 3, \ldots, M. \quad (6)$$

where cls_i is the class token, and $h_i \in \mathbb{R}^d (1 \leq i \leq M-1)$ is the hidden embedding feature output from the layer L_i.

During training, the domain-shared prompt continuously learns domain generalized knowledge across all domains. In order to prevent the domain-shared prompt from forgetting information about old domains, we introduce an inter-domain alignment constraint between the domain-shared prompt at current stages and the previous incremental stage P_{pre}:

$$\mathcal{L}_{\text{IDA}} = 1 - \frac{1}{L \times d} \sum_{i=1}^{N} \frac{p^i_{\text{shared}} \cdot p^i_{\text{pre}}}{\|p^i_{\text{shared}}\| \cdot \|p^i_{\text{pre}}\|}, \quad (7)$$

$\mathcal{L}_{\text{IDA}}$ enhances the ability to learn unified cross-domain feature representations of domain-shared prompt by matching the distribution of them across domains, reducing knowledge loss caused by domain distribution shiftS, and enabling the model to better leverage knowledge from old domains for learning in new domains.

Meanwhile, we introduce an intra-domain orthogonal constraint between the domain-shared prompt and domain-specific prompt to guide them to focus respectively on the learning of general feature representation and individual domain distribution:

$$\mathcal{L}_{\text{IDO}} = \frac{1}{L \times d} \sum_{i=1}^{N} \frac{p^i_{\text{shared}} \cdot p^i_{\text{specific}}}{\|p^i_{\text{shared}}\| \cdot \|p^i_{\text{specific}}\|}. \quad (8)$$

Supervision under $\mathcal{L}_{\text{IDO}}$ constraint, domain-specific prompt can focus on learning the unique domain distribution information of each domain to facilitate the model in adapting to new domains and preserve this domain characteristic information incorporated into the prompt bank for subsequent inference.

Finally, we can predict the relative depth map $\mathbf{d}_{rel}$ by the frozen pre-trained model f with the learnable complementary domain prompt $\mathbf{P}_{comp}$:

$$\mathbf{d}_{rel} = f(I, \mathbf{P}_{comp}) \quad (9)$$

3.4 S^2-Adapter

Furthermore, to convert the relative depth map into metric depth map, it is necessary to capture the depth space variations across domains. Here, we decouple the depth space variations into two factors: depth scale and depth shift. The depth scale factor controls the scaling relationship from the relative depth map to the metric depth map, while the depth shift factor indicates the shift between each pixel to the accurate depth value. These two factors are widely used in multi-domain learning to obtain a unified depth representation by metric depth $\hat{\mathbf{d}}$ and stabilize the multi-domain learning process:

$$\mathbf{d}_{rel} = \frac{\hat{\mathbf{d}} - t(\hat{\mathbf{d}})}{s(\hat{\mathbf{d}})}, \quad (10)$$

where $t(\hat{\mathbf{d}}) = \text{median}(\hat{\mathbf{d}})$, and $s(\hat{\mathbf{d}}) = \sum |\hat{\mathbf{d}} - t(\hat{\mathbf{d}})|$. So we can obtain the metric depth map by reversing this process:

$$\hat{\mathbf{d}} = s(\hat{\mathbf{d}})\mathbf{d}_{rel} + t(\hat{\mathbf{d}}). \quad (11)$$

However, as $s(\hat{\mathbf{d}})$ and $t(\hat{\mathbf{d}})$ are unavailable, a direct thought is to estimate them by learning a global scale factor w and shift factor b:

$$\hat{\mathbf{d}} = w\mathbf{d}_{rel} + b. \quad (12)$$

Furthermore, due to the potential inaccuracies in the relative depth maps predicted by pre-trained models, a global scale factor and shift factor may not be enough to capture the depth space variations. Therefore, we design a lightweight S^2-Adapter which consists of a scale adapter and a shift adapter to learn pixel-wise scale matrix and shift matrix respectively. In practice, we implement each adapter by two convolutional layers with 1 × 1 kernel size, followed by the formulation to obtain the final metric depth map:

$$\boldsymbol{W}_{scale} = ReLU(\boldsymbol{W}_{1,2}(ReLU(\boldsymbol{W}_{1,1}(\mathbf{d}_{rel})))), \quad (13)$$

$$\boldsymbol{W}_{shift} = \boldsymbol{W}_{2,2}(ReLU(\boldsymbol{W}_{2,1}(\mathbf{d}_{rel}))), \quad (14)$$

$$\hat{\mathbf{d}} = \boldsymbol{W}_{scale}\mathbf{d}_{rel} + \boldsymbol{W}_{shift}, \quad (15)$$

where $W_{i,j}$ means the j-th weight of the i-th adapter. We employ $ReLU$ activation function to ensure that $\boldsymbol{W}_{scale}$ is positive, while $\boldsymbol{W}_{shift}$ is not subject to this constraint. Finally, we can predict the metric depth map through the S^2-Adapter:

$$\hat{\mathbf{d}} = S^2\text{-Adapter}(\mathbf{d}_{rel}) \quad (16)$$

And due to the various depth scales in different domains, we use the Scale-Invariant Loss [1] to learn depth knowledge:

$$\mathcal{L}_{\text{Depth}} = \alpha\sqrt{\frac{1}{T}\sum_{i} g_i^2 - \frac{\lambda}{T^2}\left(\sum_{i} g_i\right)^2}, \tag{17}$$

where $g_i = \log \mathbf{d}_i - \log \hat{\mathbf{d}}_i$ and $\mathbf{d}_i$ denotes the ground truth depth map, and T denotes the number of pixels with valid depth values. We empirically set the α and λ to 10 and 0.15 respectively.

Finally, the overall loss $\mathcal{L}$ on each domain is:

$$\mathcal{L} = \mathcal{L}_{\text{Depth}} + \beta\mathcal{L}_{\text{IDO}} + \gamma\mathcal{L}_{\text{IDA}}, \tag{18}$$

where the hyper-parameter β and γ is empirically set to 1 and 10 respectively.

3.5 Domain Prompt Generation

In the inference phase, we devise complementary domain prompt generation to analyze the content of input images to select the corresponding domain-specific prompt and S^2-adapter.

In detail, we first extract image features $f_{image} \in \mathbb{R}^{h \times w \times d}$ via a query function that is implemented by the frozen pre-trained model. Then we flatten f_{image} and all domain-specific prompt respectively to get $f'_{image} \in \mathbb{R}^{h*w*d}$ and $f'^{i}_{prompt} \in \mathbb{R}^{N*l*d}$ to compute the inner product between these features and get the domain identity k by:

$$k \leftarrow \underset{i}{\text{argmax}}(f'_{image} \cdot \left(f'^{i}_{prompt}\right)^{T}). \tag{19}$$

Consequently, based on this domain identity k, we can generate the complementary domain prompt and inject it into the model. Additionally, we can select the S^2-Adapter based on the domain identity k. Thus, the corresponding complementary domain prompt and the S^2-Adapter are accurately selected to guide the model for depth predictions.

4 EXPERIMENTS

4.1 Experimental Setup

Datasets. We evaluate our method on 12 benchmark datasets, including 2 indoor and 10 outdoor datasets with different characteristics. The details of them are given in Table 1, and the data augmentation strategies are described in the supplementary material.

Implementation details. We implement experiments on PyTorch and train with RTX 3090 GPU with the AdamW optimizer for 10 epochs in each domain. We use a batch size of 8 and a one-cycle policy schedule for adjusting the learning rate with a max learning rate of 0.0000161. We use the dpt-hybrid-based model from work [29] as our backbone. We evaluate our method with 5 metrics: relative mean absolute error (AbsRel); Root Mean Squared Error (RMSE); threshold accuracy $\delta_{1.25}$; Average metrics and Forgetting metrics. The Average Metric represents the generalization capability of the model and is calculated by the mean value of the RMSE metric across all domains in the final incremental session. The Forgetting Metric assesses the ability of the model against forgetting and represents the difference between the RMSE metric of the first domain after all training stages and its value after the completion of the first stage of training.

Table 1: Details of datasets involved in the experiments.

Datasets	Characteristic	Range (m)	#Samples (Train/Test)
NYU_v2 [35]	Indoor	0~10	50K/0.6k
ScanNet [8]	Indoor	0~6	50k/17k
KITTI [38]	Outdoor	0~80	85k/1k
vKITTI_v2 [4]	Synthetic	0~80	12k/0.6k
Cityscapes [7]	Outdoor	0~200	2.9k/0.5k
CS_Foggy [32]	Foggy	0~200	8.9k/1.5k
CS_Rainy [13]	Rainy	0~200	9.5k/1.1k
DAOD [45]	Outdoor	0~120	174k/7.7k
D_Sunny [45]	Sunny	0~120	0.4k/0.1k
D_Cloudy [45]	Cloudy	0~120	0.4k/0.1k
D_Foggy [45]	Foggy	0~120	0.4k/0.1k
D_Rainy [45]	Rainy	0~120	0.4k/0.1k

Incremental domain sequences. We design 4 incremental domain sequences to comprehensively validate the performance of the model:

1. **NYU_v2→ScanNet→KITTI.** In this sequence, the depth range varies cross-domain (10m→6m→80m). Therefore, this sequence is primarily employed to assess the adapting capacity of models to depth space variations.
2. **vKITTI_v2→KITTI→CityScapes.** The primary focus of this sequence is to assess the model's capacity to adapt to image style variations, such as from virtual to real scenes.
3. **CityScapes→CS_Foggy→CS_Rainy.** In this sequence, the weather conditions in each domain are different. Therefore, training under this sequence can verify the capability of models to mitigate domain distribution shifts.
4. **DAOD→D_Sunny→D_Cloudy→D_Foggy→D_Rainy.** Due to the extreme imbalance of the sample numbers across domains in this sequence, this sequence can test the model's adaptability and resistance to forgetting in long-term few-shot scenarios.

Comparisons methods. We compare DSSP against our baseline, the classical incremental learning method (EWC [17]), and the SOTA incremental monocular depth estimation method (LL-MonoDepth [11]) under the above four incremental domain sequences. To evaluate the performance of our baseline, we train it through continuous fine-tuning (FT) and joint-domain training (JDT). We implement the classical incremental learning method EWC [17] based on our backbone. To reproduce the results of the LL-MonoDepth, we retain 500 replay samples for it in each domain, consistent with the original paper. Notably, due to the insufficient number of training samples under other weather conditions in DAOD dataset, we randomly retain 10% of the training samples for replaying in these domains.

4.2 Quantitative Results

Comparisons under different depth ranges and image styles. As illustrated in Table 2, DSSP achieves superior performance under all incremental domain sequences. Specifically, in the first sequence, compared to the SOTA methods, DSSP exhibits a significant improvement in the Average metric, demonstrating that our model

Table 2: The quantitative comparison with SOTA methods on three incremental settings which include "NYU_v2→ScanNet→KITTI", "vKITTI_v2→KITTI→CityScapes" and "CityScapes→CityScapes_Foggy→CityScapes_Rainy".

Methods	NYU_v2			ScanNet			KITTI			Average ↓	Forgetting ↓
	AbsRel ↓	RMSE ↓	$\delta_{1.25}$ ↑	AbsRel ↓	RMSE ↓	$\delta_{1.25}$ ↑	AbsRel ↓	RMSE ↓	$\delta_{1.25}$ ↑		
FT	2.210	5.161	0.656	2.494	3.748	0.426	0.194	4.361	74.707	4.423	4.759
JDT [29]	2.091	5.260	0.028	1.702	3.169	0.079	0.260	5.048	4.492	15.018	-
EWC [17]	2.304	5.367	0.674	2.497	3.776	0.424	0.191	4.323	77.758	4.489	4.960
LL-MonoDepth [11]	0.224	0.810	56.675	0.259	0.526	52.580	0.193	11.365	66.792	4.234	0.277
DSSP (Ours)	0.276	0.716	56.528	0.120	0.247	86.083	0.216	4.795	66.469	**1.919**	**0.255**

Methods	vKITTI_v2			KITTI			CityScapes			Average ↓	Forgetting ↓
	AbsRel ↓	RMSE ↓	$\delta_{1.25}$ ↑	AbsRel ↓	RMSE ↓	$\delta_{1.25}$ ↑	AbsRel ↓	RMSE ↓	$\delta_{1.25}$ ↑		
FT	6.474	42.982	0.161	1.968	33.161	5.818	17.008	16.927	54.934	31.023	39.900
JDT [29]	1.449	14.064	1.447	0.190	4.331	77.576	21.448	13.711	90.434	10.702	-
EWC [17]	4.791	37.422	0.604	1.613	28.243	9.512	17.020	15.751	59.803	27.139	34.251
LL-MonoDepth [11]	0.354	9.376	44.932	0.407	15.059	23.887	10.753	45.718	20.320	23.384	5.171
DSSP (Ours)	1.119	7.909	13.590	0.131	4.517	86.379	22.503	17.464	52.625	**9.963**	**4.279**

Methods	CityScapes			CityScapes_Foggy			CityScapes_Rainy			Average ↓	Forgetting ↓
	AbsRel ↓	RMSE ↓	$\delta_{1.25}$ ↑	AbsRel ↓	RMSE ↓	$\delta_{1.25}$ ↑	AbsRel ↓	RMSE ↓	$\delta_{1.25}$ ↑		
FT	24.300	14.213	89.352	24.959	14.224	89.455	3.726	10.259	92.062	12.898	-1.506
JDT [29]	19.539	16.731	56.898	26.241	16.445	57.310	2.847	15.218	51.943	16.131	-
EWC [17]	14.964	16.226	58.889	14.626	15.924	59.147	3.032	14.798	53.804	**15.649**	**-1.450**
LL-MonoDepth [11]	10.440	16.819	68.531	10.781	15.957	69.962	5.379	24.115	56.459	18.964	-0.389
DSSP (Ours)	27.851	17.274	59.645	12.775	15.210	61.360	3.789	16.364	48.647	16.282	-0.295

effectively mitigates the influence of the depth space variations through S^2-Adapters. In the second sequence, benefiting from our complementary domain prompt, DSSP is capable of learning unified feature representations across domains while also acquiring individual domain distributions for each domain. Therefore DSSP can maintain superior performance in both Average and Forgetting metrics. In the third sequence, none of the methods exhibited any occurrence of forgetting (i.e., forgetting metrics are less than 0). This indicates that under this scenario, the domain shift induced by weather variations is not as much as in the former two sequences, thereby enabling satisfactory performance through direct fine-tuning (FT).

Figure 4 illustrates a comparison between our DSSP and other methods across all domains and shows the final results. It can be observed that nearly all methods produce satisfactory depth map predictions in the last domain (KITTI). Notably, benefiting from complementary domain prompt, which alleviates the effects of domain distribution shifts, DSSP maintains extraordinary performance in all domains. Meanwhile, owing to the inclination of this incremental sequence to validate the model's adaptability across varying depth ranges, our model, facilitated by S^2-Adapter, exhibits the capacity to adapt depth space variations. For instance, within the first two indoor datasets, our model exhibits a relatively accurate measure of the depth of distant objects. The qualitative results under the other three additional incremental settings are provided in the supplementary material.

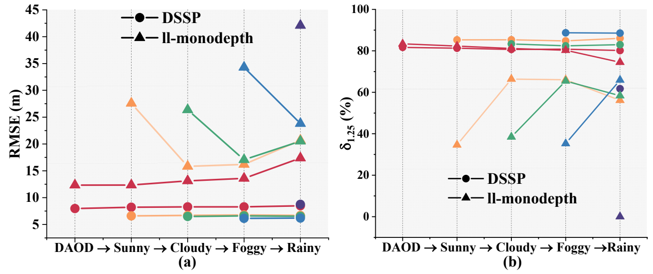

Figure 3: Comparative analysis of DSSP and the SOTA incremental monocular estimation methods (LL-MonoDepth) on mitigating forgetting performance under the few-shot DAOD incremental setting.

Comparisons under the long-term few-shot scenario. Here, we conduct experiments on long-term few-shot scenarios, where the model is required to adapt 5 domains with different weathers. And the training samples of new domains are only 400. Figure 3 describes the performance curve of different methods during training. As one can observe, DSSP is more stable and achieves better performance in each session. As illustrated in Table 3, DSSP achieves outstanding performance compared with other methods. Compared with EWC, DSSP obtains an improvement of 2.569 in terms of average RMSE over all domains. We also notice that DSSP is slightly inferior to EWC in terms of forgetting rate. Because EWC unfrozes the large-scale pre-trained model with additional regularization. Such a paradigm consumes plenty of time and computational resources and may destroy the pre-trained knowledge. Compared with the SOTA incremental depth estimation method LL-MonoDepth, DSSP obtains significant improvements in terms of Average and Forgetting metrics. The superior performance can be attributed to two

Table 3: The quantitative results on "DAOD→D_Sunny→D_Cloudy→D_Foggy→D_Rainy" incremental settings.

Methods	DAOD			DAOD_Sunny			DAOD_Cloudy			DAOD_Foggy			DAOD_Rainy			**Average** ↓	**Forgetting** ↓
	AbsRel ↓	RMSE ↓	$\delta_{1.25}$ ↑	AbsRel ↓	RMSE ↓	$\delta_{1.25}$ ↑	AbsRel ↓	RMSE ↓	$\delta_{1.25}$ ↑	AbsRel ↓	RMSE ↓	$\delta_{1.25}$ ↑	AbsRel ↓	RMSE ↓	$\delta_{1.25}$ ↑		
FT	0.320	9.045	27.116	0.365	9.506	13.992	0.392	9.980	8.563	0.345	10.331	14.391	0.306	10.322	28.224	9.837	0.080
JDT [29]	0.330	8.944	23.696	0.367	9.273	13.310	0.395	9.609	8.820	0.355	10.653	13.296	0.307	10.097	29.566	9.715	-
EWC [17]	0.313	9.013	28.951	0.359	9.391	15.315	0.381	9.898	9.739	0.340	10.311	15.209	0.302	10.733	30.288	9.869	**-0.212**
LL-MonoDepth [11]	0.170	17.379	74.500	0.333	20.694	56.131	0.325	20.523	58.340	0.263	23.806	65.896	0.999	42.089	0.000	24.898	5.045
DSSP (ours)	0.177	8.494	80.171	0.130	6.681	86.041	0.165	6.534	82.974	0.148	6.186	88.570	0.226	8.754	61.708	**7.330**	0.524

folds. Firstly, our domain-shared prompt can learn the universality across domains in feature spaces, reducing the domain gap during incremental learning. Secondly, S^2-Adapter and domain-specific prompt can learn and store the domain distribution, improving the adaptability of the model for each domain.

4.3 Ablation Studies

Shared and Specific Prompt. We first examine our DSSP by replacing domain-shared prompt and domain-specific prompt respectively. As illustrated in Table 4 (*w/o* $\boldsymbol{P}_{shared}$ *and w/o* $\boldsymbol{P}_{specific}$). The model suffers from serious forgetting problems when the model can only learn unified feature representations between domains and lacks domain-specific knowledge which demonstrates the enhancing effect of domain-specific prompt on the adaptability of the model.

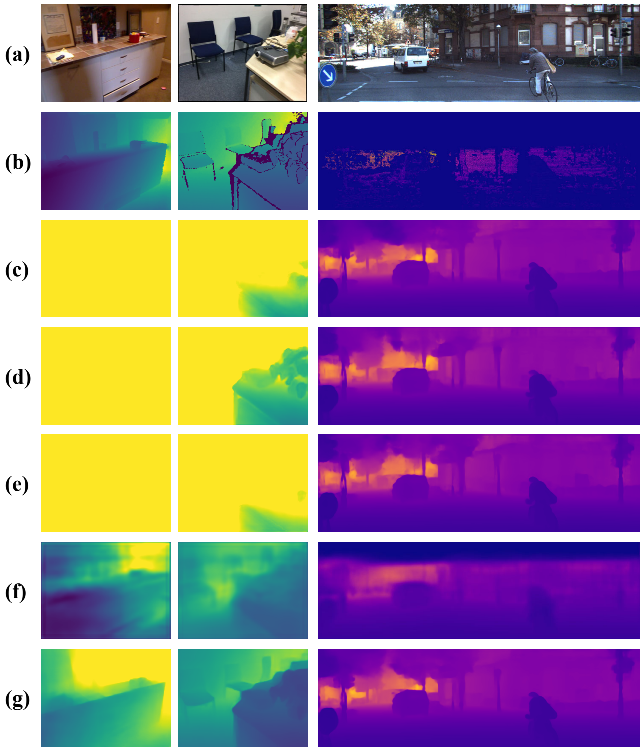

Figure 4: Qualitative comparison with SOTA methods in the learning order of NYU-v2 → ScanNet → KITTI. (a) RGB. (b) Ground truths. (c) FT. (d) JDT. (e) EWC. (f) LL-MonoDepth. (g) Ours.

S^2**-Adapter**. Then, we access the performance of our DSSP without the S^2-Adapter. As shown in Table 4 (*w/o* S^2*-Adapter*), the absence of the S^2-Adapter leads to the lack of capability of adapting the depth space variations thereby producing the severe forgetting problem.

Regularization Loss. We further validate the effects of the constraints imposed on domain-shared prompt and domain-specific prompt. As demonstrated in Table 4 (*w/o* $\mathcal{L}_{IDO}$*, w/o* $\mathcal{L}_{IDA}$ *and w/o all* $\mathcal{R}$), the absence of either constraint leads to a decrease in the model's generalization ability and resilience to forgetting. Specifically, the lack of inter-domain alignment constraint for domain-shared prompt hinders the learning of unified feature representations across domains, thereby failing to ease domain gaps, ultimately resulting in severe forgetting phenomena. Similarly, the absence of intra-domain orthogonality constraint for both types of prompts induces knowledge interference during learning, preventing domain-specific prompt from acquiring individual domain distribution information, thereby impeding the model's adaptation to new domains and weakening its generalization capability.

The length of the Prompt. In Figure 5, we validate the effect of prompt length on "NYU-v2 → ScanNet → KITTI" task. As one can observe, the best Average is achieved when the prompt length is 300. The best Forgetting is achieved when the prompt length is 250. For considerations of storage and efficiency, we adopt a default prompt length of 100.

4.4 Domain Identity Prediction Results.

Then we study the prediction accuracy of domain identity by our method. As shown in Figure 6, our method achieves good performance under the "NYU_v2, ScanNet, KITTI" sequences which demonstrates that our domain-specific prompt can learn the individual domain distribution information. Meanwhile, due to the small number of samples in the DAOD incremental sequences, our method can accurately predict the majority of domains to which the samples belong.

Table 4: The ablation studies of each components in DSSP on NYU_v2->ScanNet->KITTI incremental setting.

Methods	NYU_v2			**Average** ↓	**Forgetting** ↓
	AbsRel ↓	RMSE ↓	$\delta_{1.25}$ ↑		
w/o $\mathbf{P}_{shared}$	0.175	0.577	73.221	1.670	-
w/o $\mathbf{P}_{specific}$	1.658	3.750	8.153	2.776	3.173
w/o S^2-Adapter	3.360	6.978	0.628	3.884	5.178
w/o $\mathcal{L}_{\text{IDO}}$	0.481	1.028	31.066	5.042	0.586
w/o $\mathcal{L}_{\text{IDA}}$	1.558	3.316	2.768	5.663	2.869
w/o all $\mathcal{R}$	1.187	2.477	5.504	5.823	2.036
Ours	0.276	0.716	56.528	**1.919**	**0.255**

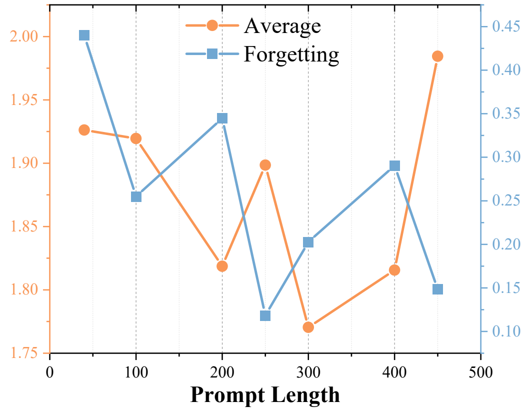

Figure 5: Effect of the length of our complementary domain prompt measured by the Average and Forgetting metrics in the learning order of NYU-v2 → ScanNet → KITTI.

4.5 Ablation of the Incremental Domain Orders

Due to varying degrees of inter-domain gaps, different incremental domain orders may result in diverse results. Consequently, we evaluate the performance of our method across all sequences on three datasets: NYU_v2, ScanNet, and KITTI. The performance of our method under different sequences on other datasets and detailed results of metrics are presented in the supplementary material. As shown in Figure 7, due to the substantial disparity in depth range between the KITTI dataset and other indoor datasets, training a model solely on KITTI and subsequently on other datasets leads to significant performance degradation (a)(f). However, when the model has been pre-trained on any indoor dataset, its performance on the KITTI dataset remains stable or even improves (b)(d).

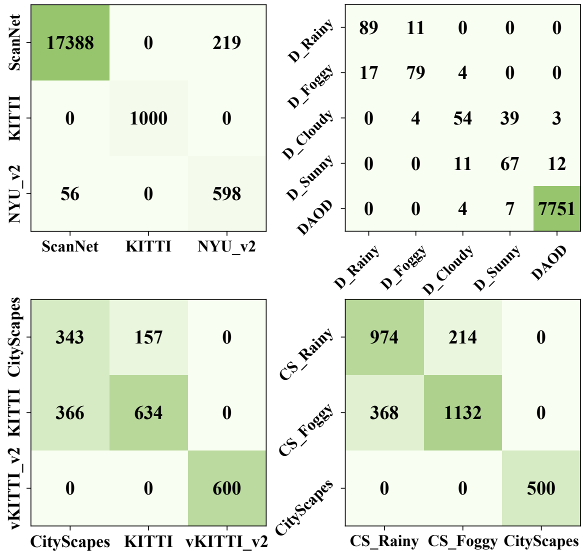

	ScanNet	KITTI	NYU_v2
ScanNet	17388	0	219
KITTI	0	1000	0
NYU_v2	56	0	598

	D_Rainy	D_Foggy	D_Cloudy	D_Sunny	DAOD
D_Rainy	89	11	0	0	0
D_Foggy	17	79	4	0	0
D_Cloudy	0	4	54	39	3
D_Sunny	0	0	11	67	12
DAOD	0	0	4	7	7751

	CityScapes	KITTI	vKITTI_v2
CityScapes	343	157	0
KITTI	366	634	0
vKITTI_v2	0	0	600

	CS_Rainy	CS_Foggy	CityScapes
CS_Rainy	974	214	0
CS_Foggy	368	1132	0
CityScapes	0	0	500

Figure 6: The accuracy of the domain identity predictions on four incremental sequences. The horizontal axis represents our prediction results, and the vertical axis represents the true domain identity.

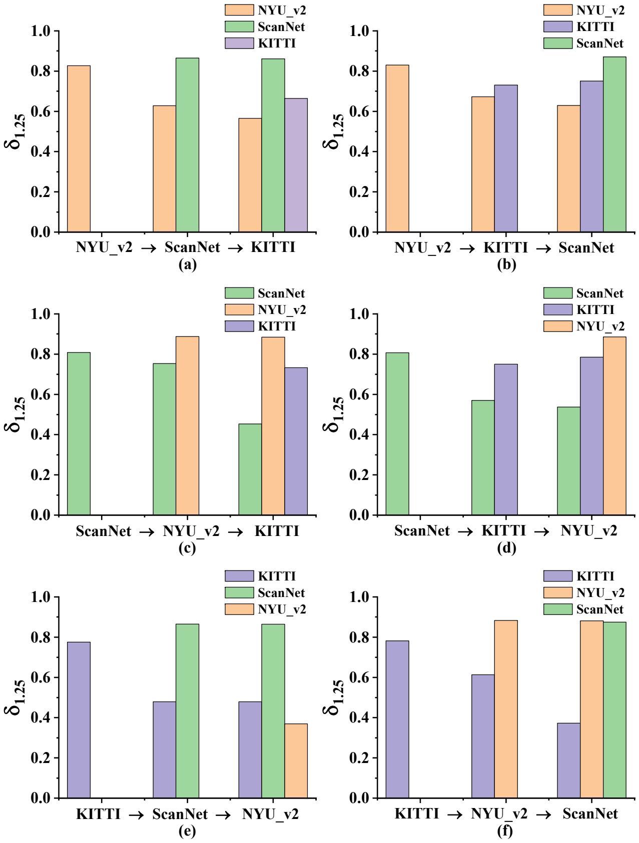

Figure 7: The $\delta_{1.25}$ accuracy of DSSP under different incremental domain orders of NYU_v2, ScanNet and KITTI datasets.

5 CONCLUSION

In this paper, we develop the DSSP for incremental monocular estimation without data privacy and security concerns, which designs complementary domain prompt and S^2-Adapter to mitigate domain distribution shifts and depth space variations. Specifically, we first generate the complementary domain prompt by learning domain shared and specific prompt which are supervised by the inter-domain alignment and intra-domain orthogonal constraint to facilitate the model to predict a unified depth representation. Then, we design a lightweight S^2-Adapter that quantizes the depth variations into scaling and shifting, enhancing the ability of the model to capture the mapping from unified depth representations to metric depth space and eventually predict the metric depth map. Extensive experiments on 12 public datasets under four different incremental scenarios demonstrate the superiority of DSSP.

We design four incremental domain sequences to provide a comprehensive benchmark for incremental monocular depth estimation. In the future, we will validate the forgetting issue and the transfer ability of our DSSP on larger depth estimation pre-trained models.

REFERENCES

[1] Shariq Farooq Bhat, Ibraheem Alhashim, and Peter Wonka. 2021. Adabins: Depth estimation using adaptive bins. In *Proceedings of the IEEE/CVF Conference on Computer Vision and Pattern Recognition*. 4009–4018.

[2] Zalán Borsos, Mojmir Mutny, and Andreas Krause. 2020. Coresets via bilevel optimization for continual learning and streaming. *Advances in neural information processing systems* 33 (2020), 14879–14890.

[3] Daniel Brignac, Niels Lobo, and Abhijit Mahalanobis. 2023. Improving Replay Sample Selection and Storage for Less Forgetting in Continual Learning. In *Proceedings of the IEEE/CVF International Conference on Computer Vision*. 3540–3549.

[4] Yohann Cabon, Naila Murray, and Martin Humenberger. 2020. Virtual kitti 2. *arXiv preprint arXiv:2001.10773* (2020).

[5] Arslan Chaudhry, Marcus Rohrbach, Mohamed Elhoseiny, Thalaiyasingam Ajanthan, Puneet K Dokania, Philip HS Torr, and Marc'Aurelio Ranzato. 2019. On tiny episodic memories in continual learning. *arXiv preprint arXiv:1902.10486* (2019).

[6] Hemang Chawla, Arnav Varma, Elahe Arani, and Bahram Zonooz. 2024. Continual Learning of Unsupervised Monocular Depth from Videos. In *Proceedings of the IEEE/CVF Winter Conference on Applications of Computer Vision*. 8419–8429.

[7] Marius Cordts, Mohamed Omran, Sebastian Ramos, Timo Rehfeld, Markus Enzweiler, Rodrigo Benenson, Uwe Franke, Stefan Roth, and Bernt Schiele. 2016. The cityscapes dataset for semantic urban scene understanding. In *Proceedings of the IEEE conference on computer vision and pattern recognition*. 3213–3223.

[8] Angela Dai, Angel X Chang, Manolis Savva, Maciej Halber, Thomas Funkhouser, and Matthias Nießner. 2017. Scannet: Richly-annotated 3d reconstructions of indoor scenes. In *Proceedings of the IEEE conference on computer vision and pattern recognition*. 5828–5839.

[9] Huan Fu, Mingming Gong, Chaohui Wang, Kayhan Batmanghelich, and Dacheng Tao. 2018. Deep ordinal regression network for monocular depth estimation. In *Proceedings of the IEEE conference on computer vision and pattern recognition*. 2002–2011.

[10] Clément Godard, Oisin Mac Aodha, Michael Firman, and Gabriel J Brostow. 2019. Digging into self-supervised monocular depth estimation. In *Proceedings of the IEEE/CVF international conference on computer vision*. 3828–3838.

[11] Junjie Hu, Chenyou Fan, Liguang Zhou, Qing Gao, Honghai Liu, and Tin Lun Lam. 2023. Lifelong-MonoDepth: Lifelong Learning for Multi-Domain Monocular Metric Depth Estimation. *arXiv preprint arXiv:2303.05050* (2023).

[12] Junjie Hu, Mete Ozay, Yan Zhang, and Takayuki Okatani. 2019. Revisiting single image depth estimation: Toward higher resolution maps with accurate object boundaries. In *2019 IEEE winter conference on applications of computer vision (WACV)*. IEEE, 1043–1051.

[13] Xiaowei Hu, Chi-Wing Fu, Lei Zhu, and Pheng-Ann Heng. 2019. Depth-attentional features for single-image rain removal. In *Proceedings of the IEEE/CVF Conference on computer vision and pattern recognition*. 8022–8031.

[14] Lam Huynh, Phong Nguyen-Ha, Jiri Matas, Esa Rahtu, and Janne Heikkilä. 2020. Guiding monocular depth estimation using depth-attention volume. In *Computer Vision–ECCV 2020: 16th European Conference, Glasgow, UK, August 23–28, 2020, Proceedings, Part XXVI 16*. Springer, 581–597.

[15] Jinyoung Jun, Jae-Han Lee, Chul Lee, and Chang-Su Kim. 2022. Depth map decomposition for monocular depth estimation. In *European Conference on Computer Vision*. Springer, 18–34.

[16] Haeyong Kang, Rusty John Lloyd Mina, Sultan Rizky Hikmawan Madjid, Jaehong Yoon, Mark Hasegawa-Johnson, Sung Ju Hwang, and Chang D Yoo. 2022. Forget-free continual learning with winning subnetworks. In *International Conference on Machine Learning*. PMLR, 10734–10750.

[17] James Kirkpatrick, Razvan Pascanu, Neil Rabinowitz, Joel Veness, Guillaume Desjardins, Andrei A Rusu, Kieran Milan, John Quan, Tiago Ramalho, Agnieszka Grabska-Barwinska, et al. 2017. Overcoming catastrophic forgetting in neural networks. *Proceedings of the national academy of sciences* 114, 13 (2017), 3521–3526.

[18] Dharshan Kumaran, Demis Hassabis, and James L McClelland. 2016. What learning systems do intelligent agents need? Complementary learning systems theory updated. *Trends in cognitive sciences* 20, 7 (2016), 512–534.

[19] Iro Laina, Christian Rupprecht, Vasileios Belagiannis, Federico Tombari, and Nassir Navab. 2016. Deeper depth prediction with fully convolutional residual networks. In *2016 Fourth international conference on 3D vision (3DV)*. IEEE, 239–248.

[20] Seokju Lee, Francois Rameau, Sunghoon Im, and In So Kweon. 2022. Self-supervised monocular depth and motion learning in dynamic scenes: Semantic prior to rescue. *International Journal of Computer Vision* 130, 9 (2022), 2265–2285.

[21] Jiaqi Li, Yiran Wang, Zihao Huang, Jinghong Zheng, Ke Xian, Zhiguo Cao, and Jianming Zhang. 2023. Diffusion-augmented depth prediction with sparse annotations. In *Proceedings of the 31st ACM International Conference on Multimedia*. 2865–2876.

[22] Zhizhong Li and Derek Hoiem. 2017. Learning without forgetting. *IEEE transactions on pattern analysis and machine intelligence* 40, 12 (2017), 2935–2947.

[23] David Lopez-Paz and Marc'Aurelio Ranzato. 2017. Gradient episodic memory for continual learning. *Advances in neural information processing systems* 30 (2017).

[24] Rémi Marsal, Florian Chabot, Angelique Loesch, William Grolleau, and Hichem Sahbi. 2024. MonoProb: Self-Supervised Monocular Depth Estimation with Interpretable Uncertainty. In *Proceedings of the IEEE/CVF Winter Conference on Applications of Computer Vision*. 3637–3646.

[25] James L McClelland, Bruce L McNaughton, and Randall C O'Reilly. 1995. Why there are complementary learning systems in the hippocampus and neocortex: insights from the successes and failures of connectionist models of learning and memory. *Psychological review* 102, 3 (1995), 419.

[26] Michael McCloskey and Neal J Cohen. 1989. Catastrophic interference in connectionist networks: The sequential learning problem. In *Psychology of learning and motivation*. Vol. 24. Elsevier, 109–165.

[27] Luigi Piccinelli, Christos Sakaridis, and Fisher Yu. 2023. iDisc: Internal Discretization for Monocular Depth Estimation. In *Proceedings of the IEEE/CVF Conference on Computer Vision and Pattern Recognition*. 21477–21487.

[28] René Ranftl, Alexey Bochkovskiy, and Vladlen Koltun. 2021. Vision transformers for dense prediction. In *Proceedings of the IEEE/CVF international conference on computer vision*. 12179–12188.

[29] René Ranftl, Katrin Lasinger, David Hafner, Konrad Schindler, and Vladlen Koltun. 2020. Towards robust monocular depth estimation: Mixing datasets for zero-shot cross-dataset transfer. *IEEE transactions on pattern analysis and machine intelligence* 44, 3 (2020), 1623–1637.

[30] Matthew Riemer, Ignacio Cases, Robert Ajemian, Miao Liu, Irina Rish, Yuhai Tu, and Gerald Tesauro. 2018. Learning to learn without forgetting by maximizing transfer and minimizing interference. *arXiv preprint arXiv:1810.11910* (2018).

[31] Andrei A Rusu, Neil C Rabinowitz, Guillaume Desjardins, Hubert Soyer, James Kirkpatrick, Koray Kavukcuoglu, Razvan Pascanu, and Raia Hadsell. 2016. Progressive neural networks. *arXiv preprint arXiv:1606.04671* (2016).

[32] Christos Sakaridis, Dengxin Dai, and Luc Van Gool. 2018. Semantic foggy scene understanding with synthetic data. *International Journal of Computer Vision* 126 (2018), 973–992.

[33] Joan Serra, Didac Suris, Marius Miron, and Alexandros Karatzoglou. 2018. Overcoming catastrophic forgetting with hard attention to the task. In *International conference on machine learning*. PMLR, 4548–4557.

[34] Reza Shokri and Vitaly Shmatikov. 2015. Privacy-preserving deep learning. In *Proceedings of the 22nd ACM SIGSAC conference on computer and communications security*. 1310–1321.

[35] Nathan Silberman, Derek Hoiem, Pushmeet Kohli, and Rob Fergus. 2012. Indoor segmentation and support inference from rgbd images. *ECCV (5)* 7576 (2012), 746–760.

[36] Zhenbo Song, Jianfeng Lu, Yazhou Yao, and Jian Zhang. 2021. Self-supervised depth completion from direct visual-LiDAR odometry in autonomous driving. *IEEE Transactions on Intelligent Transportation Systems* 23, 8 (2021), 11654–11665.

[37] Libo Sun, Wei Yin, Enze Xie, Zhengrong Li, Changming Sun, and Chunhua Shen. 2022. Improving monocular visual odometry using learned depth. *IEEE Transactions on Robotics* 38, 5 (2022), 3173–3186.

[38] Jonas Uhrig, Nick Schneider, Lukas Schneider, Uwe Franke, Thomas Brox, and Andreas Geiger. 2017. Sparsity invariant cnns. In *2017 international conference on 3D Vision (3DV)*. IEEE, 11–20.

[39] Arnav Varma, Hemang Chawla, Bahram Zonooz, and Elahe Arani. 2022. Transformers in self-supervised monocular depth estimation with unknown camera intrinsics. *arXiv preprint arXiv:2202.03131* (2022).

[40] Niclas Vödisch, Kürsat Petek, Wolfram Burgard, and Abhinav Valada. 2023. CoDEPS: Online continual learning for depth estimation and panoptic segmentation. *arXiv preprint arXiv:2303.10147* (2023).

[41] Chenyang Wang, Junjun Jiang, Xingyu Hu, Xianming Liu, and Xiangyang Ji. 2024. Enhancing Consistency and Mitigating Bias: A Data Replay Approach for Incremental Learning. *arXiv preprint arXiv:2401.06548* (2024).

[42] Zizhang Wu, Zhuozheng Li, Zhi-Gang Fan, Yunzhe Wu, Jian Pu, and Xianzhi Li. 2023. V2Depth: Monocular Depth Estimation via Feature-Level Virtual-View Simulation and Refinement. In *Proceedings of the 31st ACM International Conference on Multimedia*. 688–697.

[43] Ke Xian, Chunhua Shen, Zhiguo Cao, Hao Lu, Yang Xiao, Ruibo Li, and Zhenbo Luo. 2018. Monocular relative depth perception with web stereo data supervision. In *Proceedings of the IEEE Conference on Computer Vision and Pattern Recognition*. 311–320.

[44] Mengqi Xue, Haofei Zhang, Jie Song, and Mingli Song. 2022. Meta-attention for vit-backed continual learning. In *Proceedings of the IEEE/CVF Conference on Computer Vision and Pattern Recognition*. 150–159.

[45] Guorun Yang, Xiao Song, Chaoqin Huang, Zhidong Deng, Jianping Shi, and Bolei Zhou. 2019. Drivingstereo: A large-scale dataset for stereo matching in autonomous driving scenarios. In *Proceedings of the IEEE/CVF Conference on Computer Vision and Pattern Recognition*. 899–908.

[46] Wei Yin, Chi Zhang, Hao Chen, Zhipeng Cai, Gang Yu, Kaixuan Wang, Xiaozhi Chen, and Chunhua Shen. 2023. Metric3d: Towards zero-shot metric 3d prediction from a single image. In *Proceedings of the IEEE/CVF International Conference on Computer Vision*. 9043–9053.

[47] Wei Yin, Jianming Zhang, Oliver Wang, Simon Niklaus, Simon Chen, Yifan Liu, and Chunhua Shen. 2022. Towards accurate reconstruction of 3d scene shape from a single monocular image. *IEEE Transactions on Pattern Analysis and Machine Intelligence* 45, 5 (2022), 6480–6494.

[48] Jaehong Yoon, Divyam Madaan, Eunho Yang, and Sung Ju Hwang. 2021. Online coreset selection for rehearsal-based continual learning. *arXiv preprint arXiv:2106.01085* (2021).

[49] Huangying Zhan, Ravi Garg, Chamara Saroj Weerasekera, Kejie Li, Harsh Agarwal, and Ian Reid. 2018. Unsupervised learning of monocular depth estimation and visual odometry with deep feature reconstruction. In *Proceedings of the IEEE conference on computer vision and pattern recognition*. 340–349.

[50] Chaoqiang Zhao, Gary G Yen, Qiyu Sun, Chongzhen Zhang, and Yang Tang. 2020. Masked GAN for unsupervised depth and pose prediction with scale consistency. *IEEE Transactions on Neural Networks and Learning Systems* 32, 12 (2020), 5392–5403.

[51] Jiquan Zhong, Xiaolin Huang, and Xiao Yu. 2023. Multi-Frame Self-Supervised Depth Estimation with Multi-Scale Feature Fusion in Dynamic Scenes. In *Proceedings of the 31st ACM International Conference on Multimedia*. 2553–2563.

[52] Tinghui Zhou, Matthew Brown, Noah Snavely, and David G Lowe. 2017. Unsupervised learning of depth and ego-motion from video. In *Proceedings of the IEEE conference on computer vision and pattern recognition*. 1851–1858.